LOW-TEMPERATURE BRITTLENESS OF IRON AND STEELS

KITAJIMA, Kazunori
Research Institute for Applied Mechanics, Kyushu University : Professor

出版情報：Reports of Research Institute for Applied Mechanics. 22 (70), pp.61-87, 1975. 九州大学応用力学研究所
バージョン：
権利関係：

Reports of Research Institute for Applied Mechanics
Vol. XXII, No. 70, 1975

LOW-TEMPERATURE BRITTLENESS OF IRON AND STEELS

By

Kazunori KITAJIMA*

A review is made of the recent research on fundamental mechanisms in the brittle fracture of iron and steels. The process of brittle fracture may consist of a number of stages ranging from microscopic to macroscopic dimensions, i.e., the stages of atomic dimensions, of the order of a grain size and the region of crystalline aggregates.

In the stage of atomic dimensions, the ductility of a crystal lattice is attributed to the balance between nucleation of cleavage cracks and dislocation loops under the given state of stress and is characterized quantitatively by the manitude of the ratio σ_{th}/τ_{th} relative to the ratio σ_{max}/τ_{max}, where σ_{th} and τ_{th} are the critical normal and shear stresses of the crystal lattice, and σ_{max} and τ_{max} are the maximum normal and shear stresses operating in the cleavage and slip planes, respectively. The lattice ductility of iron is then discussed with relation to deformation of the BCC lattice and the nature of covalent-type bonding associated with unpaired d electrons in BCC transition metals.

As far as the role of plastic deformation in the mechanism of brittle fracture is concerned, the high lattice resistance of screw dislocations characteristic of BCC metals is responsible for the high yield stress at low temperatures or high strain rates, and the low lattice resistance of edge dislocations for the piling-up and coalescence of edge dislocations at the yield stress. On the other hand, the easy cross slip of screw dislocations can relieke local stress concentrations.

Experimental evidence on the initiation and propagation of cleavage cracks in single crystals of iron is critically reviewed from the above viewpoint. In particular, the growth of plastic deformation associated with the propagation of cleavage cracks at high velocities is attributed to the nucleation of dislocations at the tip of the crack. The activation energy of the nucleation of dislocations obtained experimentally is compared with that predicted theoretically, $k_s\sigma_{th}(\tau_{th}/\sigma_{th}-\tau_{max}/\sigma_{max})$. This gives an estimate $\sigma_{th}/\tau_{th}\simeq 0.8\ \sigma_{max}/\tau_{max}$ at the tip of the crack, where σ_{max}/τ_{max} has the approximate value of five.

The effects of solid-solution alloying elements on the ductility of iron are discussed from the standpoint of lattice ductility and plastic deformation.

A review is presented for the phenomenological theories treating the initiation and propagation of cleavage cracks in an area of about one grain

* Professor, Reserch Institute for Applied Mechanics, Kyushu University.
This paper is translated from the proceeding of International Symposium Toward Improved Ductility and Toughness (The Iron and Steel Institute of Japan, and The Japan Institute of Metals, 1971, Kyoto) p. 143.

size. Next the differences in fracture characteristics of steels are explained on the basis of the role of the size and form of the precipitated particles.

Finally, some critical comments are made on the mechanisms relating microscopic and macroscopic processes, in particular, fracture stress, propagation of macro-cracks and the problem of size effects.

1. Introduction

Steel is a well known material widely used for structures and machines because of its excellent toughness characterized by high yield stress, high tensile strength and high ductility. On the other side, it is sometimes liable to brittleness by loading at low temperature or high strain rate, and the problem has been an important technological theme from the stand point of safety usage of structures.

In general various modes of brittle fractures of iron and steels can be classified into two main types from the difference in underlying mechanisms, *i.e.* the one is the cleavage type fracture and the other is the grain boundary brittleness. In the later, a small amount of impurity atoms segregated at grain boundary play a dominant role as found in grain boundary brittleness of pure iron or temper brittleness of low alloy steels containing Ni and Cr. Recent progresses in this type of fracture was reviewd by Low, [1] so that we shall omit this problem from the present treatment.

As for the cleavage fracture of iron and steels, the fundamental theme may be to answer the question why BCC iron is so liable to cleavage at low temperature. Then the effects of various alloying elements, solid solution or precipitations, and grain size on the characteristics of cleavage fracture are to be reasonably explained based on the settlement of the fundamental problem.

Recognition of large discrepancy between theoretical and measured values of tensile strength of crystals was the first step to the study of fracture. Griffith [2] introduced the conception of pre-existing crack. Besides, in earlier times, macroscopic behaviour of fracture was descrived by the continium mechanics. Ludik and Davidenkov [3] developed the phenomenological theories based on the conceptions of nominal critical fracture stress and flow stress, and succeeded in explanations for fracture stresses and transition temperatures of steels including effects of notches. The line of thought has been further developed to recent fracture dynamics [4] introducing the conception of plastic work associated with propagation of crack [5], which provide important measure for brittleness of steels from technological stand-point.

On the other hand, atomistic approach to the mechanisms of cleavage fracture was started by Zener [6] and Mott [7], who reconsiled the theoretical value of tensile strength to the empirical ones by showing microscopic stress concentration induced by pile up of dislocations is responsible for nucleation of crack in metals. The theory was developed further by Cottrell and Petch et al. [8],[9],[10],[11], and reasonable explanations have been presented for charac-

teristics of fracture, *i.e.* effects of grain size and notches on fracture stress and transition temperature, but the various assumptions used in these theories yet lack the sound physical basis letting them remain to be a phenomenological stage.

One of the cause of brittle fracture is the large increase of the yield stress at low temperatures characteristic in iron. The atomistic mechanisms of the problem, however, essentialy solved by Hirsch [14] and Suzuki [15] who attributed the high yield stress to large Peierls stress of screw dislocation in BCC metals. The consequences of the theories are pursued on the effects of solid solutional alloying elements [16].

The other concerns with the brittleness of perfect lattice. In fact the condition of stress concentration envisaged in the pile up model not always means sufficient condition for initiation of cleavage crack, because the stress concentration might be released by nucleation of dislocation loop in some cases [17], *i.e.* we must take into account the counter-balance of nucleation of crack and dislocation loops in perfect lattice near the tip of pile up.

In general, the brittleness of perfect lattice is controlled not only by the tensile strength σ_{th} but also by the shear strength τ_{th} of the crystal. The crystal may be brittle or ductile according as the ratio τ_{th}/σ_{th} is larger or smaller than the ratio τ_{max}/σ_{max}, where τ_{max} and σ_{max} are the operative shear and normal stresses respectively. Developements along this idea were made to some different directions by Kitajima [18] and Cottrell et al. [19].

One of them is to calculate τ_{th} and σ_{th} for various crystals. Some results are obtained for Lennerd-Jones and ionic crystals [25], but no reasonable theories are yet obtained on metals particularly on BCC transition metals. Discussions will be presented in this paper to find any clues to this problem.

The other direction may be to pursue experimentally the concequences of the idea. In this paper some experinmental works made on the propagation of cleavage crack in single crystal of iron will be introduced. The effects of solid solutional elements on the fracture of iron alloys will be included in this paper, since it is not only important in technological problems but interesting from the present stand-point.

Finally we shall present a review for the inter-relations between fracture processes ranging from macroscopic to microscopic dimensions.

2. Fundamental Properties Characterizing the Brittleness of Iron

2.1. Brittleness of Crystal Lattice

The critical stress of cleavage σ_{th} of a crystal was estimated by Orowan [5]

$$\sigma_{th}=\sqrt{\frac{E\gamma}{a}},$$

where a is the lattice constant, E the Young's modulus, γ the surface energy, and the approximation is used for the normal stress σ as function of

interatomic distance u by $\sigma = \sigma_{th} \sin 2\pi u/\lambda$ and $2\gamma = \int \sigma du = \lambda\sigma_{th}/\pi$.

In the case of iron we have $\sigma_{th} = 4800\,\mathrm{Kg/mm^2}$ taking $E = 2 \times 10^{12}$ dyne $/\mathrm{cm^2}$, $\gamma = 1200$ erg/cm², and $a = 2.85$Å. The value of σ_{th} is compared to the experimental value of $\sigma_{max} \simeq 1200\,\mathrm{Kg/mm^2}$ obtained by Brenner [20] for iron whisker which contain no dislocation, and the largest tensile stress of $\sim 300\,\mathrm{Kg/mm^2}$ obtained for recent super high strength steels. Hull [21] estimated γ of W from the critical stress of propagation of a small cleavage crack pre-formed on the surface of specimen by spark in liquid nitrogen.

Theoretical considerations for the critical shear stress τ_{th} of a crystal were made by Mackenzie and Seeger [22]. When FCC lattice is sheared along the slip plane $(1\bar{1}1)$ and the direction [121], the sheared lattice take the form of nearly BCC lattice and twinned FCC lattice in the pass where the relative shear displacement of neighbouring atomic planes takes the value a/12[121] and a/6 [121] respectively.

$$\frac{a}{12}[121]+\frac{a}{12}[121]+\frac{a}{12}[21\bar{1}]+\frac{a}{12}[21\bar{1}]=\frac{a}{2}[110]$$

Mackenzie estimated $\tau_{th} \leq G/30$ from the reasoning that energy of the lattice takes minimum values in the cases of nearly BCC and twinned FCC lattice.

Similar considerations may be applied for BCC lattice, *i.e.* when the lattice is sheased along the plane $(1\bar{1}0)$ relative shear displacement of atomic plane take the path [23]

$$\frac{a}{8}[110]+\frac{a}{4}[112]+\frac{a}{8}[110]=\frac{a}{2}[111],$$

and the lattice take the form of nearly FCC lattice when the displacement is a/6[110], where lattice energy take a minimum. On the other hand, when the lattice is sheared along the plane $(11\bar{2})$ atomic displacement takes the path

$$\frac{a}{6}[111]+\frac{a}{3}[111]=\frac{a}{2}[111]$$

where a/6[111] sheared position correspond to a twinned BCC lattice where lattice energy takes a minimum value.

Calculations of σ_{th} and τ_{th} were made for lattices with inter-atomic potentials of central force type such as Lennard-Jones crystals [24)25)18)] and ionic crystals with Born-Meyer type potentials [25)26)]. Fig. 1 shows Tyson's calculations for Lennard-Jones crystal [25]. On the other hand general formulation of the problem was presented by Born [24] from the stand-point of stability of a deformed lattice. As shown in his theory, σ_{th} and τ_{th} depend on the states of stresses and the constraints of deformations [18]. An example is shown in Fig. 1c, in which τ_{th} increases with the increase of compressive normal stress σ_n acting on the slip plane [25].

Table 1 shows the characteristics of crystal lattices summarized by Kelly [25], where the measured values of E and γ, the estimated values of σ_{th}

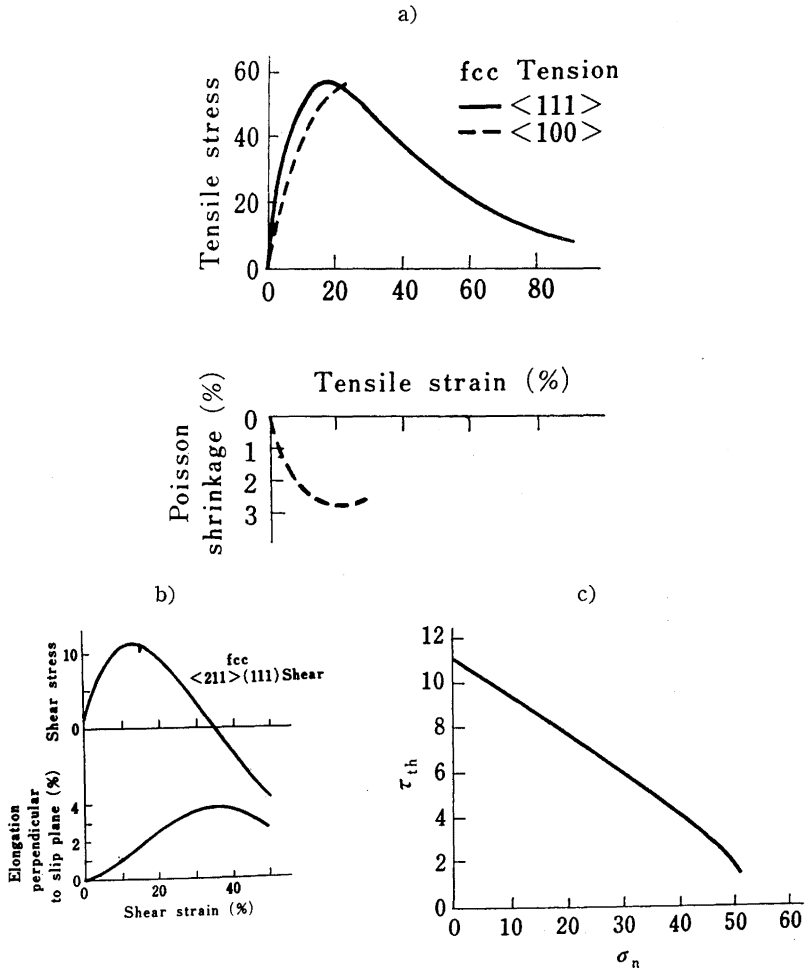

Fig. 1. Stress-strain characteristics of Lennard-Jones crystal with interatomic potential $\phi = -\frac{a}{r^6} + \frac{b}{r^{12}}$,

a) Tensile deformation, after Tyson[25].
b) Shear deformation, Tyson[25].
c) Effect of normal stress σ_n operating in slip plane on τ_{th}, Kelly et al.[25].

and τ_{th} from E and γ for metals, and the calculated values for NaCl and Diamond[25] are listed. As argued in the previous section brittleness of crystal lattice is characterized by the ratio σ_{th}/τ_{th}. When the ratio is smaller than 2 as in the cases of NaCl and Diamond, the lattice is brittle under simple tension, where $\sigma_{max}/\tau_{max} = 2$. On the other hand, when the ratio is larger than 5~6 as in the cases of FCC metals, the lattice is ductile even under sharp notch test, where $\sigma_{max}/\tau_{max} = 5$~6 near the tip of the notch.

Table 1. Calculated values of σ_{th} and τ_{th}, after Kelly et al.[25], a_0, γ, E' and G' were determined by extrapolating experimental values to 0°K. σ_{th} and τ_{th} for metals were calculated using the assumptions $\sigma_{th}=\left(\frac{E'\gamma}{a_0}\right)^{1/2}$, $\frac{\tau_{th}}{G'}=0.04$ (fcc), or 0.11 (bcc).

	Lattice constant a_0(Å)	E' $\left(\frac{10^{11}\text{dyne}}{\text{cm}^2}\right)$	Surface energy γ(erg-cm^{-2})		σ_{th} $\left(\frac{10^{11}\text{dyne}}{\text{cm}^2}\right)$	$\frac{\sigma_{th}}{E'}$	G' $\left(\frac{10^{11}\text{dyne}}{\text{cm}^2}\right)$	$\frac{\tau_{th}}{G'}$	τ_{th} $\left(\frac{10^{11}\text{dyne}}{\text{cm}^2}\right)$	$\frac{\sigma_{th}}{\tau_{th}}$
			Measured	Extrapolated						
Cu	1.80	7.5	1730at 1000°C	3630	3.87	0.51	3.43	0.04	0.137	28.2
Ag	2.03	4.9	1130at 925°C	2930	2.66	0.54	2.20	0.04	0.088	30.2
Au	2.04	4.63	1350at 1000°C	3250	2.73	0.59	2.02	0.04	0.081	33.8
Ni	1.76	15.00	1725at 1455°C	4300	6.05	0.41	6.85	0.04	0.274	22.1
W	3.16	40.48	6300at 77°C	6415	9.08	0.22	16.35	0.11	1.80	5.04
			2900at 2000°C	7650						
α-Fe	2.85	14.33	1940at 1450°C (δ-iron)	4520	4.79	0.34	6.48	0.11	0.71	6.75
Diamond	1.54	120.9			14.0	0.116	50.5	0.25	12.1	1.16
NaCl	2.75	5.75	118at 25°C	140	0.38	0.067	2.48	0.164	0.406	0.94

BCC metals are the critical cases, in the meaning that they are ductile under simple tension test but nearly brittle under sharp notch test since σ_{th}/τ_{th} is 5~6 in these metals as seen in Table 1. The above discussions, however, are limitted to the case of temperature 0°K. At finite temperatures we must consider the effects of thermal vibration of lattice. Based on the Peierls model Kitajima [18] calculated the activation energies of nucleation of crack and dislocation loop in high stresses near σ_{th} and τ_{th}, which are shown to be smaller than those of classical models of Griffith's crack and perfect dislocation loop.

2.2. Brittleness of BCC transition metals

Calculations of σ_{th} and τ_{th} for BCC transition metals are very difficult at the present stage because of lack of precise knowledges for electronic structures of the metals [27] particularly concerning for cohesive energies of lattices at finite deformations. But some inspections may be possible base on some appropriate approximations.

Johnson [28] proposed a method of calculation for BCC lattice, where central force is assumed for inter-atomic forces but cutting off the interactions between atoms separated further than second neighbour pairs, and applied to the problem of lattice defects, Chang [29] applied Johnson's method to the calculation of bonding near the edge of a crack in BCC and FCC lattice of iron, and showed that BCC lattice is more brittle than FCC lattice. However, we must point out the importance of the roles of non-central force, which are characteristic in BCC transition metals and not taken into account in these calculations.

It is well-known experimental facts that BCC Alkali metals of the group I_a do not show brittleness, and BCC transition metals of the group V_a, such as V, Nb and Ta, show less brittleness than those of the group VI_a, Cr, Mo and W, and the group $VIII_a$, Fe. The differences in brittleness among the BCC metals, maight be explained taking into account the roles of non-central force, *i.e.* covalent like bonding due to unpaired electrons in d cell characteristic in BCC transitions metals. The type of bonding in the group I_a Alkali metals is purely metalic one, *i.e.* bonding by free electron, and the BCC lattice structure of the metals is attributed to the larger entropy of BCC lattice compared with that of FCC lattice which reduces the free energy. On the other hand unpaired electrons in d cell having the wave function with octa-poles tend to form covalent like bondings between atoms in BCC lattice, which contribute much to cohesive energy of the lattice. And this is considered to be the main reason why the transition metals take the BCC lattice structure [30]. We may then easily deduce that the covalent like bonding have larger contribution to τ_{th} than the free electron bonding, since the later is insensible for shear deformation which accompany no volume change of the lattice, while the both types of bondings contribute to σ_{th} since tensile deformation accompany the volume change of the lattice.

From the above reasoning we may deduce that the brittleness of the lattice may increase as the number of unpaired electrons in d cell of the atom increase. Since the number of unpaired electrons is 3, 5 and 4 for V (d^3s^2), Cr (d^5s^1) and Fe (d^6s^2) in the group V_a, VI_a and $VIII_a$ respectively, the brittleness may be least in V, largest in Cr and intermediate in Fe. However the deduction is too simple when we take into account the fact that tha states of d electrons in the lattice is very different from those in a free atom, *i.e.* they show band structure and not localized to a specific atom. The precise nature of d electrons in cohesive energy problem is yet unsolved at the present stage particularly for interactions between electrons, including those between d band and s band, though the tendency of localization of d electrons and associated covalent like bonding is supposed to be large[31]. So that the above deduction is confined to a qualitative one.

As for the cohesive energy problem we must cite the semi-empirical theory proposed by Engel and Brewer[32]. They determined the transition of the states of electons in forming lattice structure, *i.e.* they estimated the binding energies per electron of s, p and d in the lattice, particularly change of binding energy associated with the transition of states of electrons from d state to s or p states, from the measured values of binding energies. They deduced the criterion of transitions by the condition of minimizing the tolal energy of the system, thus obtained the results, for instance V ($d^{3\cdot5}sp^{0\cdot5}$), Cr ($s^{4\cdot5}p^{0\cdot5}$) and Fe ($d^{6\cdot5}sp^{0\cdot5}$). Moreover they assumed the type of lattice is determined by the total number of s and p electrons and not by the states of d electrons. (We may point out the last deduction contradicts with the one of electronic theory mentioned above.) Their explanations for the cohesive energy and type of lattice for transition metals is interesting and succeeded in predictions for lattice type of various metals and alloys. Leslie[33] presented a explanation for the brittleness of Fe alloys based on this theory. The details of his explanation with the criticisms will be stated in later section.

2.3. Roles of Plastic deformation in brittleness of iron.

We may point out the three factors as for the roles of plastic deformation in the mechanisms of brittle fracture of BCC metals, *i.e.* (1) increase of yield stress at low temperatures, (2) the concentration of stress associated with the inhomogenuity of plastic deformation, and (3) the relaxation of stress concentration due to nature of plastic deformation.

The large increase of yield stress with the decrease of temperature or increase of strain rate characteristic in BCC metals is one of the main causes of brittleness in the meaning that the high stress level make the initiation and propagation of cleavage crack easy to occur. The increase of the yield stress had been attributed to the locking of dislocations by interstitial impurity atoms, such as carbon and nitrogen, but recently was explained as an intrinsic character of dislocation in BCC lattice by Hirsch and Suzuki.

Hirsch [14] attributed the large barrier against the slip of screw dislocation to the constriction of extended dislocation required to make movement in slip planes {110} or {112} since the a/2<111> screw is expected to extend on the 3 twin planes of {112} and the planes of {110} in the stational state. On the other hand Suzuki [15] attributed the large Peierls potential of the screw dislocation to the large cyclic change of core energy of screw dislocation for successive movements of one atomic distance on the slip plane {110} with its axis parallel to <111>, *i.e.* arrangement of atoms in the three neighbouring atomic rows in the core of screw dislocation take the screw arrangement with equal distance separation in a lattice position, where core energy is very low, but it takes the enforced symmetrical arrangement in the neighbouring lattice position, where each atoms in the three atomic rows are forced to come to the same axial positions in the core of screw dislocation consequently core energy is very high, in movement on the slip plane {110}. Hirsch's theory have the merits in explanations for the experimental facts that the critical shear stress on the slip plane {112} depend generally on the operative direction of the shear stress, and explanation for the characteristics of cross slip. However, the size of extension of the dislocation assumed is smaller than one atomic distance, consequently theoretical background is not yet so firmly established. On the contrary, Suzuki's theory is clear in theoretical base, but it over-estimates the Peierls stress by factor of about.10 based on simple atomic force calculations, and can not give explanations for the experimental facts mentioned above. More consistent theory unifying the merits of two theories may wait further studies, [75] but we may say that the essential part was solved by the two theories on the cause of high yield stress at low temperature characteristic in BCC metals.

The two theories predict further that the Peierls stress of edge dislocation is very small compared with that of screw dislocation in accordance with the experimental facts [13]. Then we may deduce that the edge dislocations can pile up accompanying high stress concentration even under the stress where screw dislocation just start to move. The concentration of stress may initiate cleavage crack under suitable conditions. Cottrell's immobile dislocation [9] formed by the reaction of two (110) systems of edge dislocation, $a/2[\bar{1}\bar{1}1] + a/2[111] \rightarrow a[001]$, may supply the barrier against the pile up.

The stress concentration and stress relaxiation accompanying slip band is higher order characteristics of plastic deformation, for which our knowledges are not yet so much accumulated. But we may mention here that, characteristics of large number of slip systems and easiness in cross-slip of screw dislocation make the stress concentration difficult in BCC metals. This prediction is consistent with the experimental facts that the slip band in BCC metals generally show diffuse structure consisting of rather homogeneously distributed very fine slip lines, and particularly wavic pattern caused by frequent cross slip at higher temperatures. According to Hirsch's theory [14], easiness of cross slip is attributed to the smallness of difference between the lattice resistances of screw dislocation on the slip plane {110} and {112}.

Twinning is, however, easy to occur in BCC lattice accompanying characteristic inhomogeneous deformation, which may cause large stress concentration connected with initiation of cleavage. Details of them will be explained in later sections.

2.4. Effects of solid solutional alloying elements on the brittleness of iron.

Following to the recent psogress in researches on pure metals, much attensions have been paid on the effects of solid solutional alloying elements on the characteristics of plastic deformation and brittleness of BCC alloys.

Interstitial [36] and substitutional [35)16)] alloying elements in BCC metals are known to induce generally softening of yield stress at low temperatures, but hardening at higher temperatures[34]. Sato and Meshii [37)38)] presented an explanation for this phenomenon taking into account linear elastic interactions between screw dislocation with large Peierls stress and the stress field around an impurity atom, and showed that the formation of kink pair is aided by the stress field. On the other hand, large Peierls stress of screw dislocation is essentialy attributed to the regular arrangement of atoms in the core of dislocation according to Suzuki's theory, then we may deduce that the factors introducing atomic size irregularity may weaken the Peierls potential [39]. Then as the strength of the barrier become larger the yield stress may increase, and cause temperature dependent type hardening and then temperature independent type hardening. The deductions were proved by experiments [39].

The solid solutional elements inducing softening, however, not always

Table 2. Charpy impact characteristics for solid-solution alloys of iron, after Leslie et al.[33].

Alloy content (%)	Crain size (ASTM No.)	Transition temperature (°C)	Maximum absorbed energy	
			(ftlb)	(kgm)
Fe	4 — 5	−34	75	10.3
Fe	0 — 2	−29	65	9.0
1.5Ni	5 — 6	−54	80	11.0
3Ni	7 — 9	−95	90	12.4
1.5Si	6 — 7	− 4	80	11.0
3Si	4 — 7	100	55	7.6
1.5Mn	6 — 8	−20	80	11.0
3Mn	7 — 9	− 7	80	11.0
1.5Cr	4 — 5	−18	75	10.3
3Cr	4 — 7	−23	75	10.3
6Cr	6 — 7	−23	85	11.7

decrease the brittleness [33], Table 2. The alloying elements (Si, Al, Cr, Mo etc.)[33], which decrease austenite range in phase diagram, are known to increase the brittleness, while the elements (Ni [40], Mn, Pt, Ir, Rh, Ru)[41] which widen the austenite range decrease the brittleness, though the effects of Cr and Mn are rather small, Table 2. Two ways of explanation for the mechanisms of these facts are presented. The one attributes the change of brittleness to change of easiness of cross slip induced by alloying elements. For instance photomicrographic appearance of slip band in 3% Si-Fe is more straight than those in pure iron, and correspondingly the transition temperature is heigher by 240°C than that of the later. On the other hand, 3 % Ni-Fe shows wavic appearance of slip band down to 50°K, which is lower by 70°K than that of pure iron, 120°K, correspondingly the transition temperature is lower by 70°C than that of pure iron. Easiness of cross slip may generally supresses the brittleness by relaxing stress concentration, but no explanations are presented for the roles of solid solutional elements on the mechanism of cross slip. Futhermore we may point out the facts that the metals of VI_a group, W and Mo, show larger brittleness than the metals of V_a group, Ta, Nb and V, though the former show easier cross slip than the later, and no correlation were found between the characteristics of flow stress and the brittleness in tensile tests of solid solutional alloys of iron [33], Fig. 2.

The other explanation is based on the idea that solid solutional elements change the brittlelness of crystal lattice itself. We shall now consider the mechanism of change of brittleness of BCC lattice by alloying. The elements

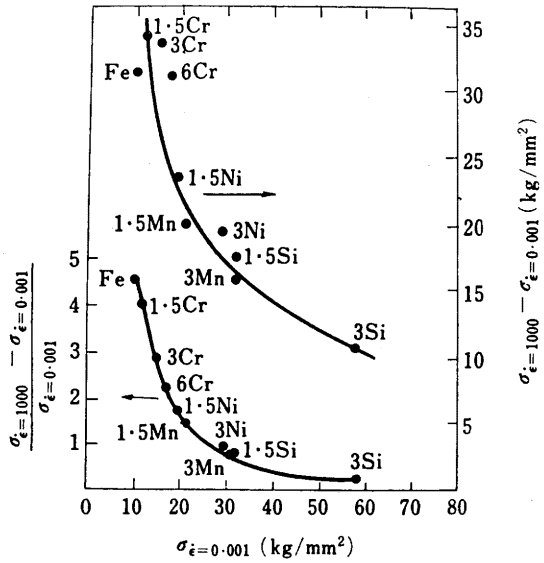

Fig. 2 Strain rate dependency of yield stress in solid solution alloys of iron, after Leslie et al.[33].

widen the austenite region in phase diagram may decrease the difference between the free energy of BCC lattice and that of FCC lattice of the same material. Then critical shear stress τ_{th} on the slip plane (110) may be lowered by decrease in difference of free energy between the unsheared BCC state and the sheared state corresponding to the displacement a/8 [110], which is very near to the FCC lattice state as explained in the previous section. According to experiments [42], the critical temperature of martensite transformation is lowered by about 300°C by alloying of 9 % Ni to iron, correspondingly the difference of free energy between α and γ phase decrease by about 0.04 eV per one atomic cell. On the other hand, the elastic energy stored in the lattice under the critical shear τ_{th} is estimated as $1/2\times\tau_{th}\times\gamma_c\times a^3\simeq 0.15$ eV per one atomic cell, where γ_c is the critical shear strain estimated as $\simeq\sqrt{6}/8$, $\tau_{th}=G/10$, $G=8\times10^{11}$ dyne/cm^2, $a=2.86$Å. Since the value of 0.04 eV is same order as the stored elastic energy estimated above, we may expect the decrease of τ_{th} by alloying of Ni in the meaning stated above. Furthermore the activation energy of propagation of cleavage crack is expressed by $k_s\sigma_{th}(\tau_{th}/\sigma_{th}-\tau_{max}/\sigma_{max})$ as will be explained in later section. Then we can see small change of τ_{th} induce rather large change of the activation energy since the later is proportional to the difference$(\tau_{th}/\sigma_{th}-\tau_{max}/\sigma_{max})$ and τ_{th}/σ_{th} is nearly equal to τ_{max}/σ_{max} at the tip of crack in BCC metals. Baced on the idea presented above, we can give reasonable explanation, in order of magnitude at least, for the experimental evidences that the transition temperature decrease to −70°C by alloying of 3 % Ni and −200°C by alloying of 9 % Ni in iron.

Leslie [33] attributed the increase of ductitity of Fe alloys to the increase of cohesive energy caused by the change of number of electrons by alloying based on Engel-Brewer's theory. According to his prediction Ni, Pt and Pd increase the cohesive energy, Mn and Cr induce small change, while Si decrease the cohesive energy in accordance with the experimental evidences.

However we may point out that the increase of cohesive energy may mean the increase of σ_{th}, but may not be linked directly to ductiltity of lattice since the latter is determined by τ_{th}/σ_{th} in the present arguments.

According to the present standpoint, the change of ductiltity of a lattice is closely related to the change of τ_{th} through the change in covalent type bondings in BCC transition metals. Details of the explanations may await developments in electronic theory, but we may deduce qualitatively that alloying of Ni; d^8s^2, Pd; d^{10} and Pt; d^8s^2 into Fe; d^6s^2 decrease the number of unpaired electrons in d state, thus decrease the covalent type bonding.

3. Processes in brittle fracture of iron and steels.

Processes in brittle fracture of iron and steels consist of a number of stages ranging from microscopic to macroscopic dimensions. These may be conveniently classified into the four stages, i.e. the stage of atomic dimension which is discussed in the previous chapter, the stage inside a grain,

that of the order of few grain sizes including grain boundaries, and that of crystalline aggregate with macroscopic dimension, each of which have characteristic mechanisms. The processes in these stages, however are closely connected with each other, and equally weighted in the characteristics of ultimate fracture.

3.1. Initiation and propagation of cleavage crack in the stage inside a grain.

The nucleation of cleavage crack may be caused by high stress concentration accompanying to the inhomogenuity of plastic deformation. Mott [7] and Stroh [8] proposed the pile up model of dislocations for initiation of crack. When n edge dislocations in a slip band are piled up against a barrier under the mean stress τ, maximum stress σ_{max} is$\sim n\tau = \tau_{max}$ at the edge of the pile up. And micro crack is nucleated when σ_{max} reach σ_{th}. Thus we obtain

$$L=\frac{Gbn}{\pi(1-\nu)\tau},\quad n\tau=\alpha'\sigma_{th},$$

where L is length of slip band and about 1/2 of grain size d, b the Burgers vector, ν the Poisson's ratio, α' the number of$\sim$1. Cottrell [9], Petch [10] and Kitajima [11] showed that the crack once initiated by Stroh's mechanism can only propagate inside a grain under the stress larger than a critical stress σ_f which depend in general on the plastic deformation produced at the tip of propagating crack, *i.e.*

$$\sigma_f=K\left(\frac{p}{\gamma}\right)^{1/2}\left(\frac{\sigma_{max}}{\tau_{max}}\right)^{1/2}\left(\frac{b}{d}\right)^{1/2}, \tag{2}$$

where p is plastic work, γ the surface energy. Assuming $p\sim 10\,\gamma$ and combining (2) with condition of yield stress presented by Petch based on experiments,

$$\tau_y=\tau_i+kd^{-1/2}, \tag{3}$$

they have succeeded in explanations for characteristics of fractur of iron and steels, *i.e.* fracture stress, transition temperature, and their dependencies on grain size, triaxiality of stresses etc..

However various assumptions used in these phenomenological theories must be re-examined based on realistic physical mechanisms. Some of them will be cited below.

The characteristics of slip band in iron explained previously is not consistent with the pile up model. Stress concentration by slip band may consist of two factors, the macroscopic one and the microscopic one due to piling up of edge dislocations in a fine slip line inside the slip band. τ_i in (3) correspond to the lattice resistance of screw dislocation, while the edge dislocations are piled up under the stress τ_y since the lattcie resistance of them are

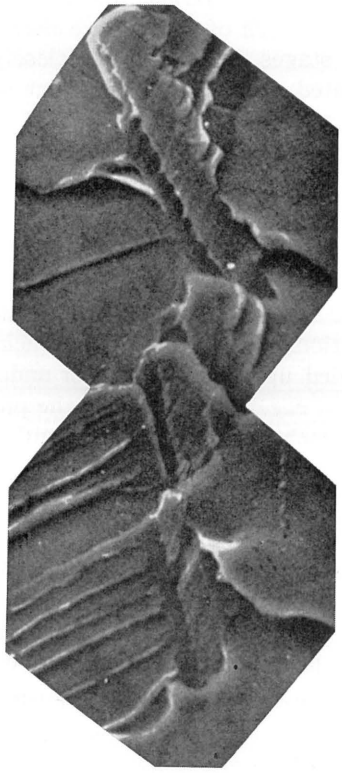

a) ×2000

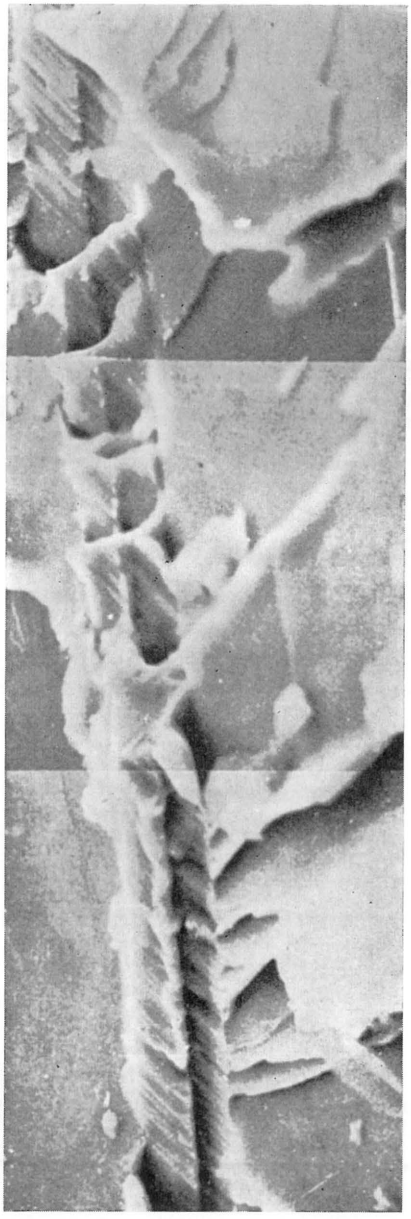

b) ×3600

Photo. 1. Scanning electron micrographs of crack origins accompanying a twin in a single crystal of pure iron.
a) Viewed along a direction not parallel to the plane of the twin.
b) Viewed along the direction parallel to the plane of the twin.
The striations inside the twin show a shear-type fracture. A straight groove is formed along the center of the twin. A series of cleavage facets start from the ends of shear fracture facets along the twin boundary. A series of segments of twin as observed in a) is proved to be placed in a single twin as shown in b). The twin is cut by cleavage planes with various heights, after Kitajima [45].

very small. Terazaki [43] discussed the initiation of crack by pile up of edge dislocations distributed in many slip lines.

According to experimental evidences on iron single crystals no cracks are found to initiate associating with slip band, but almost always initiated accompanying twin. Examples are reported on a crack associated with crossing two twin bands [44], and many cracks started from boundary of a twin band, Photo 1 [11),13),45)], for which no simple theoretical models can be applied. k in (3) had been explained by locking of dislocation by interstitial impurity atoms such as carbon, Cottrell effect, but thereafter was showen to be independent of temperatures in a well annealed specimen, where dislocations are tightly locked by precipitations of carbides [46].

3.2. Propagation of cleavage crack inside a grain

As for the mechanism of growth of plastic deformation at the tip of propagating crack two ways of explanations are presented. Friedel [47] and Tetelman [48] assumed that the dislocations pre-existing near the head of propagating crack are moved by the stress field around the tip of crack. Based on the idea Tetelman [48] estimated the plastic work due to the movements of dislocations,

$$p=\gamma[(\sqrt{5}/1.7)\rho_0^{\frac{3}{2}}b^3\ 8.8\times10^2(V_c/V)^2T^{\frac{5}{2}}], \tag{4}$$

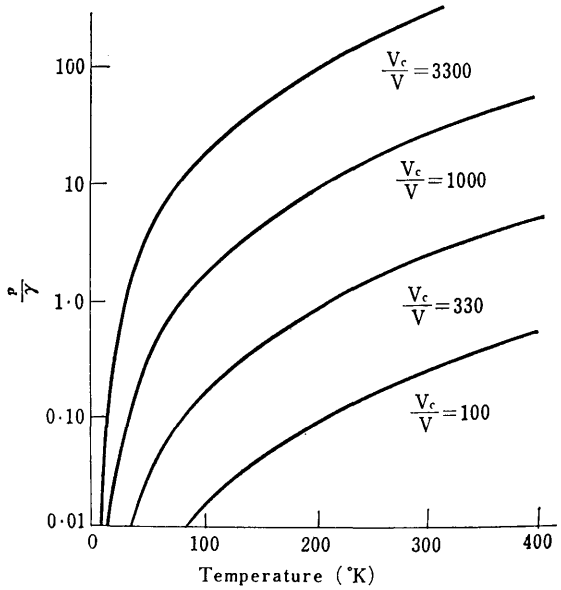

Fig. 3. Plastic work associated with the propagation of cleavage crack, calculated by Tetelman [48] using equation (4). Plastic work is caused by movement and multiplication of pre-existing dislocations near the tip of the crack.

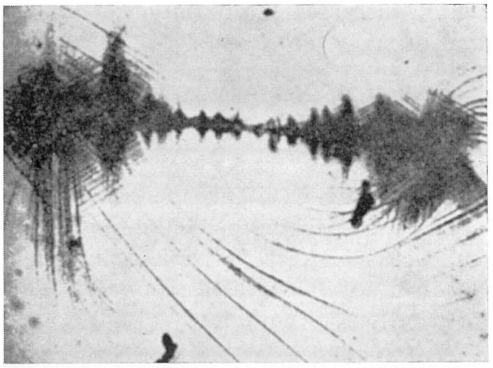

Photo. 2. Distribution of dislocations around a crack in an Fe-3%Si single crystal cathodically charged with hydrogen. Tetelman[48].

where ρ_0 is the initial density of movable Frank-Read sources, V_c the critical speed of propagation of crack, Fig. 3, Photo. 2. In this mechanism initial density of dislocation ρ_0 plays essential role in brittleness of materials. Gilman[49] emphasized the factor of multication of dislocations by double cross slip in plastic work.

On the other hand, dislocation loops as well as micro cracks may be nucleated at the tip of propagating crack when τ_{th}/σ_{th} is nearly equal to τ_{max}/σ_{max} as in the cases of BCC transition metals. Kitajima[18] estimated the plastic work due to this mechanism.

$$ln\frac{p}{K\tau_{max}b}\simeq 3ln\tau_{max}/\tau_p+\left(\frac{3kT}{A}+1\right)ln\frac{2V_c}{V}-k_s\sigma_{th}(\beta-\alpha)/kT, \qquad (5)$$

where $\beta=\tau_{th}/\sigma_{th}$, $\alpha=\tau_{max}/\sigma_{max}$ and K, A, k_s are constants. The first and 2nd terms in right hand side of (5) represent the contribution of lattice resistance of dislocation, and 3rd term that of nucleation of dislocation loops at the tip of the crack. On this mechanism the brittleness of the crystal is determined by the intrinsic properties of the lattice irrespective of the number of initial dislocations.

The former mechanism predict that the plastic work p becomes comparable with γ only when V is smaller than $V_c/100$ as shown by the equation (4) and in Fig. 3. This conclusion is not so much affected even by taking into account of the multiplication of dislocations by double cross slip[48]. Then a crack started with the velocity $V>V_c/10$ could not be stopped even at high temperatures near melting point. In the later mechanism, on the contrary, p become large at high temperatures even if the propagation speed V is larger than $V_c/10$ as shown by (5).

Experiments to test the predictions of the two theories were carried out by Kitajima[45][51]. It was concluded that the crack started with the velocity larger than $V_c/10$ in iron single crystal was stopped at temperatures of 300°C

and dislocations produced near the surface of crack were proved to be nucleated at the tip of propagating crack.

Tensile tests were performed on plate of single crystals of pure iron with the thickness 1.4 mm and the breadth of 40 mm. The one end of the specimen was cutted by a sharp notch and cooled to the liquid nitrogen temperature, while the other end was heated to about 350°C. The crack started at the notch was propagated with the velocity of$\sim$300 m/sec$>V_c/10$, and stopped at the place with the temperature of$\sim$300°C Fig. 5.

The surface of cleavage crack was then etched and examined by electron microscope, one example of which is shown in photo. 3. The etch pit densities thus determined are shown in Fig. 4. High density of dislocations, 100$\sim$1000 times larger than that of initial dislocations, were observed to be confined within the layer of the thickness of about 3 μ, which is comparable to the mean distance of initial dislocations. From these evidences it is concluded that the dislocations grown near the surface of crack was those produced by nucleation of dislocation loops at the tip of propagating crack. Activation energy of the nucleation of dislocation loop which is expressed as $k_s\sigma_{th}(\tau_{th}/\sigma_{th}-\tau_{max}/\sigma_{max})$ in the equation (5) was determined as$\sim$0.2 eV from

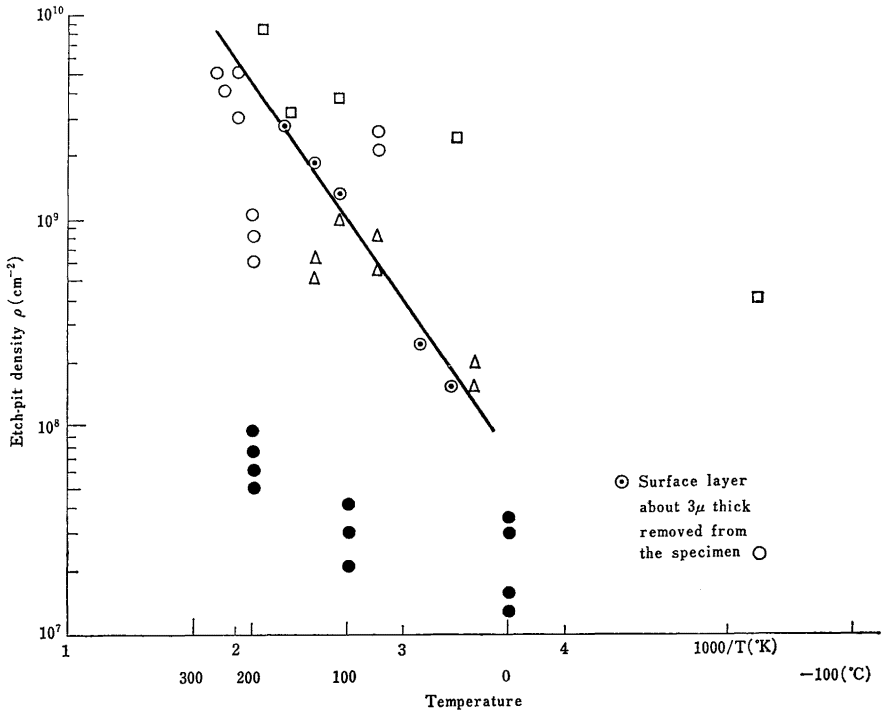

Fig. 4. Etch pit densities observed on the cleavage surface of iron single crystals, after Kitajima [45,51].

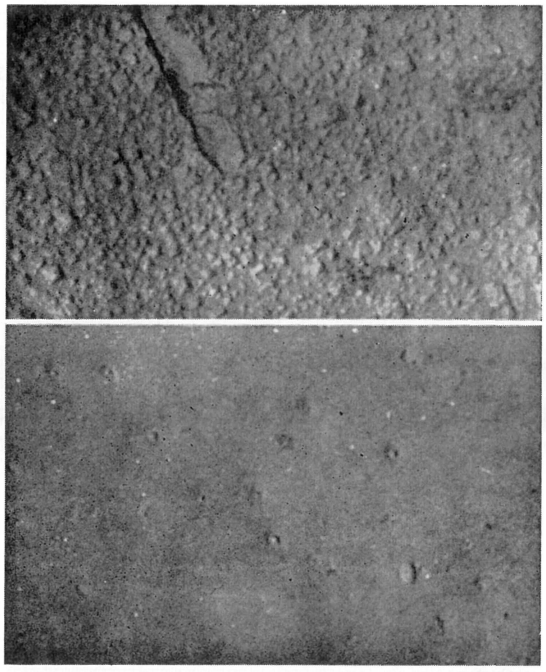

×10,000

Photo. 3, Etch-pit patterns of a surface cleaved at a temperature of about 100°C. Kitajima [45].
a) Surface as cleaved.
b) Surface after removing a 3μm layer.

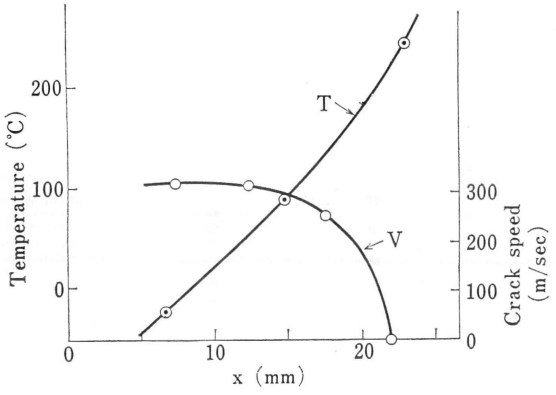

Fig. 5. Crack speed in single crystal of iron. Kitajima. [51]

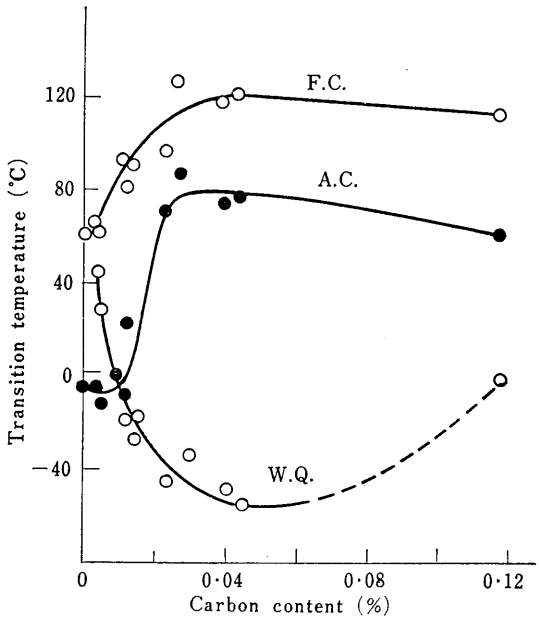

Fig. 6. Transition temperature of iron-carbon alloys measured with Charpy impact. W.Q., water quenched specimens, A.C.; air-cooled specimens, F.C.; furnace-cooled specimens. Intergranular fractures can be observed with carbon contents under 0.005%. Allen[55].

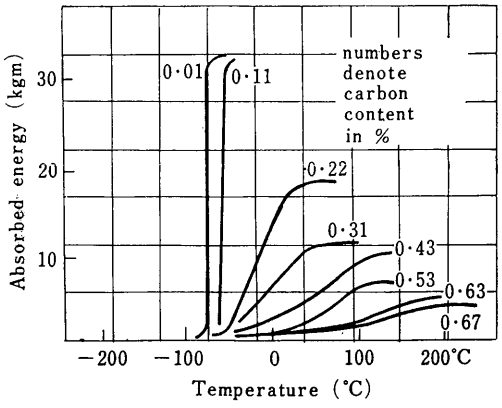

Fig. 7. Effect of temperature and carbon content of iron-carbon alloys on energy absorbed in Charpy test, after Rinebolt[54].

Fig. 4.

On the other hand using the estimated value of $k_s\sigma_{th}\simeq 1.14\ eV$ we have $(\tau_{th}/\sigma_{th}) = 1.2(\tau_{max}/\sigma_{max})$, where τ_{max}/σ_{max} is about 1/5.

On the surface of cleavage at low temperatures $<0°C$ the high intensity of twins up to $\sim 10^{9\sim 10}$ cm^{-2} were observed. These may be nucleated at the tip of crack and contribute much to plastic work. At high temperatures $>$ 100°C the surface marking lack the river pattern and resembles to ductile cleavage [52] observed near transition temperature and those in 9 % Ni steels [53] fractured at liquid nitrogen temperature.

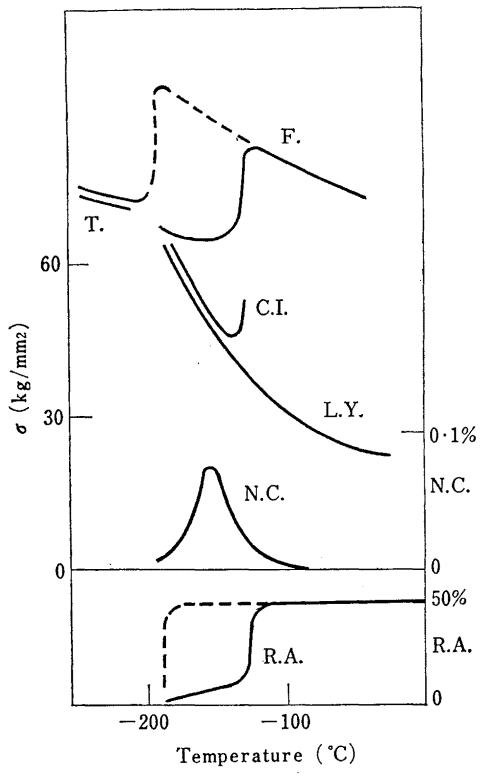

Fig. 8. Simple tensile test of low-carbon steel, Hahn et al. [57]. Steel E: 0.22% C, 0.36% Mn, furnace cooled from 1250°C with a grain size of 0.106 mm. F. =fracture stress, T. =twinning stress, C.I. =crack-initation stress, L.Y. =lower yield stress, N.C. =ratio of number of cracks stopped within the grain to number of grains, R.A. =reduction of area. The dotted line indicates the estimated characteristics of pure iron based on experimental data obtained on Steel M with 0.16% C and 1.30% Mn.

3. 3. Cleavage fracture of steels containing carbides

As for the roles of precipitations in fracture of steels, carbides provide typical example. In annealed steels containing C of 0. 02～0. 04 %, coarse plate-like carbides are precipitated along grain boundary or inside grain, and cracks are easily started from them [55)56)]. Figs. 6 and 7. The range of transition temperature is wide and high density of stopped microcracks are observed near the transition range in this type of steels. Fig. 8. In contrast to the above type, in steels containing appropriate Mn, carbides have granular forms from which cracks are difficult to start [55)], transition is very sharp and stopped micro cracks are rarely observed in this type of steels. These characteristics resemble to those in pure iron.

The difference in characteristics of fracture in the two types of steels can be explained as follows. In the former, which may be called as precipitation type, micro cracks are easily formed assisted by the stress concentration, breaking of carbides, or separation along the boundary of precipitations under relatively low stresses. But these cracks can not be propagated to long distances, probably be stopped at grain boundary, and restart only after work hardening by deformation. Fig. 9 shows the characteristics of propagation of micro cracks which are formed at the end of slip band with the length L, under various stress level of σ_{max} and various triaxiality of stresses $(\sigma_{max}/\tau_{max})$, where plastic work p is assumed to have the form $p = p_0(V_c/V)$. Each curve in Fig. 9 represents the variation of crack velocity V, ordinate $\eta = \left(\frac{V}{V_c}\right)^2$, versus the crack length C, absissae $\xi = \omega\left(3+\frac{C}{C_n}\right)$, under the initial condition characterized by $C_n = \frac{L}{2}(\tau_{max}/\sigma_{max})$ and $\omega = \frac{\gamma}{2p_0}$

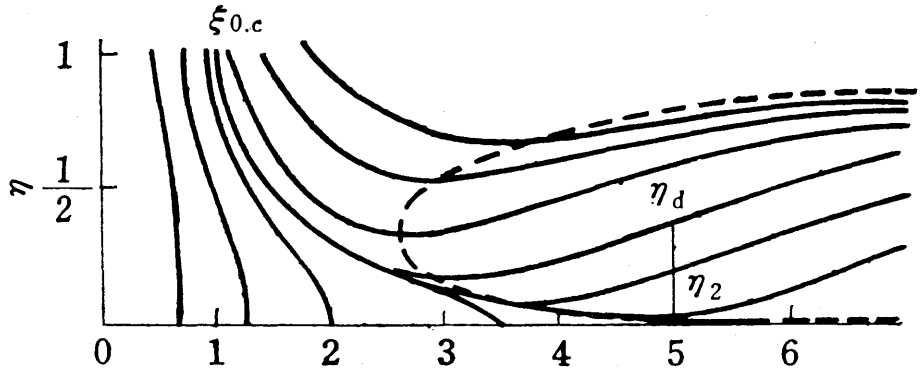

Fig. 9. Propagation of crack grown at tip of piled-up dislocations. Kitajima [18)]

$\eta=\left(\frac{V}{V_c}\right)^2$, $\varepsilon=\omega\left(3+\frac{c}{c_n}\right)$, $c_n=\frac{L}{2}\left(\frac{\tau_{\max}}{\sigma_{\max}}\right)$, $\omega=\frac{\gamma}{2p_0}\left(\frac{L}{b}\right)$ $\times\left(\frac{\tau_{\max}}{\sigma_{\max}}\right)\left(\frac{\sigma_{\max}}{\sigma_G}\right)^2$, $\sigma_G{}^2=\frac{2E\gamma}{\pi(1-\nu^2)b}$, c=length of crack.

$\times\left(\frac{L}{b}\right)\left(\frac{\tau_{max}}{\sigma_{max}}\right)\left(\frac{\sigma_{max}}{\sigma_G}\right)^2$, where $\sigma_G=\frac{2E\gamma}{\pi(1-\nu^2)b}$. It is assumed that a crack starts with the velocity $V_c, \eta=1$, at the position $C=0$, $\xi=\xi_0=3\omega_0$. As can be seen in Fig. 9, when $\xi_0=3\omega$ is smaller than a critical value $\xi_{0,c}$ cracks can not propagate to far distances, but is stopped. These may correspond to initial formation of cracks in the precipitation type steels.

On the other hand, in pure iron type such as pure iron or steels containing Mn, stress level of initiation of crack is high, corresspondingly ω is large and $\xi_0=3\omega\geqq\xi_{0,c}$ so that the crack can propagate or be re-acceralated and penetrate the barrier of grain boundary, thus the condition of fracture is given by the equation $3\omega=\xi_{0,c}$, which is no more than the equation (2).

Returning to the former case, ultimate fracture may occur after that the stress level is raized by work hardening accompanying to deformation and enable to re-start the stopped crack. The condition of the re-start of a crack once stopped at the grain boundary is given by $\sigma_f=\sqrt{\frac{Ep_b}{d}}$, where p_b is the plastic work required to penetrate the grain boundary, and has the value$\sim 10^5 erg/cm^2$ according to experiments [58)59)]. p_b may depend on the plastic deformation near the grain boundary, consequently on the nature of carbide precipitations near the boundary.

The difference of the fracture characteristics between the two types of steels can be explained by the equations (2) and (6) as shown in Fig. 10.

3.4 Work hardening and ductile fracture

The flow stress of steels σ consist of the two compornents, the tempera-

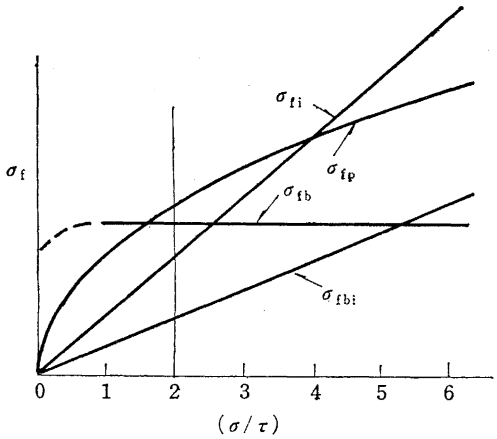

Fig. 10. Dependency of fracture stress σ_f on the triaxial ratio (σ/τ). σ_{fi}, σ_{fp}, σ_{fb} are fracture stresses calculated by equations (1), (2) and (6) respectively. σ/τ corresponds to 1 for the state of stress in torsion, 2 for simple tension and 6 for sharp notched specimens.

ture dependent part σ_i and temperature independent part σ_h. σ_i is determined essentialy by the lattice resistance of screw dislocation, while σ_h by the elastic interaction between dislocations and is proportional to square root of the density of dislocations ρ. Stain ε is related to ρ by $\varepsilon \propto \rho d$ where the slip distance is assumed to be proportional to grain size. Then we have $\sigma_h = \alpha\sqrt{\varepsilon/d}$, where α is a constant of the order of 1. More precisely, dislocation structure depends on temperature, and slip distance is restricted by precipitations, *i.e.* precipitation hardenings.

Uniform elongation ε_c is determined by the condition of plastic instability and equal to the index of work hardening n, phenomenological constant determined by the relation $\sigma = A\varepsilon^n$. ε_c is generally shown to increase slowly then decrease rapidly as the temperature decrease according to experiments[61].

Apart from the uniform elongation, reduction of area and true fracture stress are determined by the condition of ductile fracture. Ductile fracture starts by the separation at boundary of precipitates[62]. Cavities once formed are elongated by plastic deformations, where strain tend to concentrate locally as predicted by the thory[64] of rigid plastic materials, since work hardening rate is very small at large strain. Opening of cavities is accelerated by stress components of hydrostatic tension. Critical size of precipitations which is able to nucleate cavities is reported as$\sim 1\mu$[63].

3.5. Macroscopic behaviour of brittle fracture of steels

Combining the microscopic conditions for initiation of crack and plastic deformation with the continium mechanical methodologies we may obtain reasonable descriptions for the macroscopic behaviours of brittle fractur of steels. But in realistic processes many problems yet remain unsolved since macroscopic and microscopic processes are so closely related that they could not be clearly separated. In this section some of them will be cited below.

3.5.1 Condition of initiation of brittle fracture

Much varieties in characteristics of brittle fracture are well known, but the author think it may be usefull to classify these varieties from the standpoint of transition from pure iron type to precipitation type. For instance criterion of constant nominal fracture stress proved in some[65,66] cases may correspond to the precipitation type. Difficuties yet remain for the transition range where initiation of brittle fractures is preceeded by ductile fracture as observed in center of cylindrical specimen and near the root of notch (thumb nail) in notched specimens. Redistribution of stress and shocks accompanying to ductile fracture may influence initiation of brittle cracks. COD[67] may be useful measure for criterion of brittle fracture but condition of fracture may require another constants.

3.5.2 Condition of propagation of brittle fracture

Criterion for the propagation of brittle fracture is usually provided by K_c value which is related to the plastic work p by $Ep = K_c^2$. Fig. 11 shows the temperature dependence of K_c for various steels obtained by double tension tests. The activation energy of p calculated from Fig. 11 ranges 0.4-0.2 eV for steels from mild steel S25C to high tension steel HT80. These may correspond to those of static plastic deformation in various stress level since K_c is measured from stopped cracks. However p in propagating state may also be important in analysing realistic processes. Fig. 12. Little is known for the plastic processes in high speed propagation of crack. For instance, the strain rate is estimated as$\sim 10^5$/sec for the plastic deformation of 3 % confined within a layer of 0.3 mm near the tip of crack propagating with the velocity of 1000 m/sec. In such high strain rate plastic deformation may

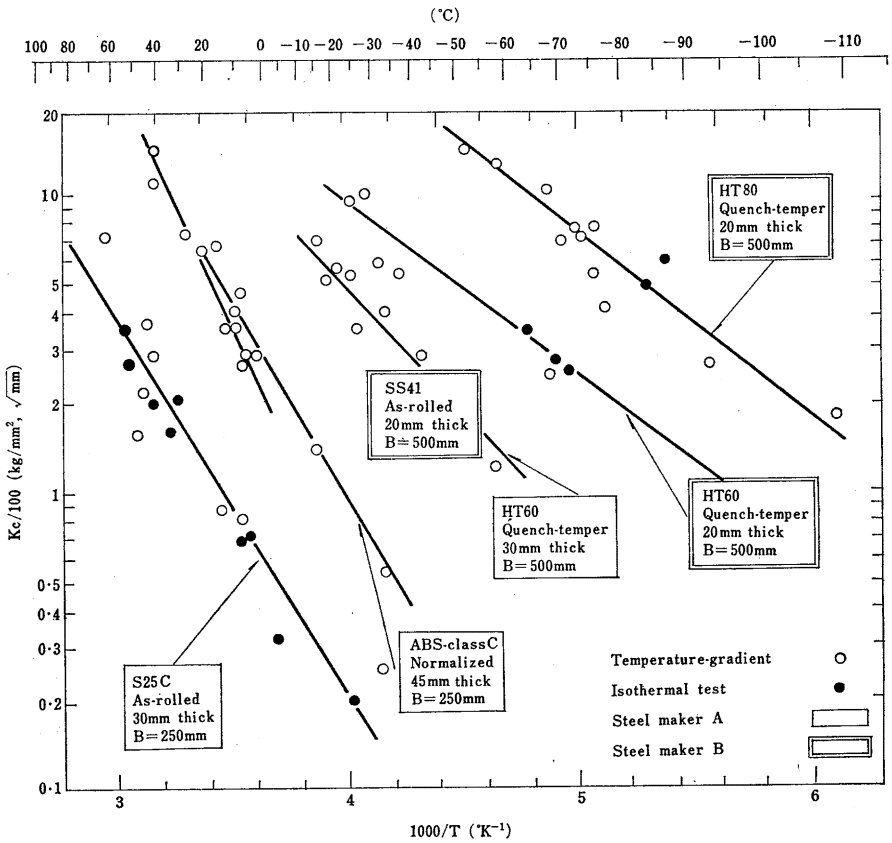

Fig. 11. Temperature dependency of K_c value of various steels obtained by double tension test. Koshiga.[69]

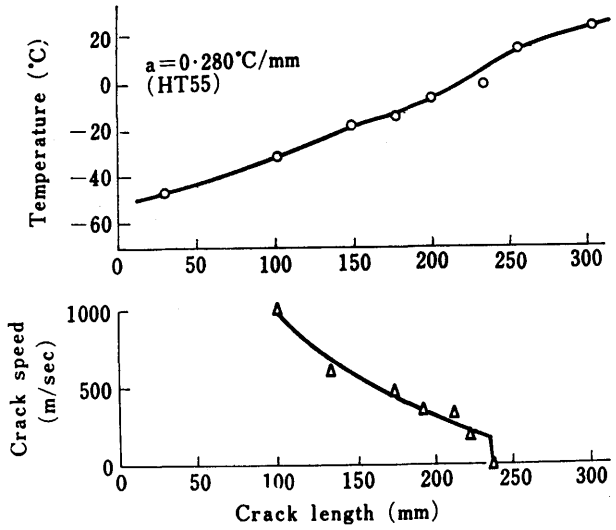

Fig. 12. Propagation velocity of crack measured on the steel plate with temperature gradient. Ikeda[70].

occur by nucleation of dislocations not by multiplication. It is reported twinning is main mode of deformation in iron at the strain rate larger than 10^5/sec. Hall explained the plastic work from the stand point of plastic wave propagation near the tip of crak. According to his theory the thickness of the plastic zone δ is given by

$$\delta = \frac{C_p}{C-C_p} \cdot \frac{C-V}{V} l ,$$

where C is velocity of elastic wave $C = \sqrt{E/\rho}$, C_p that of plastic wave $C_p = \sqrt{\frac{d\sigma}{d\varepsilon}/\rho}$, V the velocity of the crack, l the size of plastic region proceeding ahead the crak.

3.5.3 Yielding in steels and size effects in fracture.

In crystalline aggregate unit of inhomogenuity may refer to a grain size, but in steels the size of Lüders band is sometimes much larger than a grain size, and it controll the unit of inhomogenuity. For instance triaxiality near the root of the notch in steel plate depend on the magnitude of the size of Lüder's band relative to the thickness of the plate[73][74]. The same is for the size of shear lip which appear in propagation of crack in steel plate. These factors may responsible for various size effects in the initiation and propagation of brittle fracture in steels.

Reference*

1) Low, J.R., Jr.: Trans. AIME, **245** (1969), p. 2481.
2) Griffith, A.A.: Phil, Trans, Roy. Soc., **A221** (1920), p. 163.
3) Ludwik, Z.: Metallkde **15** (1924), p. 207. Davidenkov, N.N.: Dinamicheskaya Ispytania Metallov (1936), Moscow
4) Irwin, G.R.: Structural Mechanics, (Pergamon 1960, New York)
5) Orowan, E.: Rep. Prog. Phys., **12** (1949), p. 185.
6) Zener, C.: Fracturing of Metals, (ASM 1948, Cleveland) 3.
7) Mott, N.F.: Proc. Roy. Soc., **A220.** (1953), p. 1.
8) Stroh. A.N.: Proc. Roy. Soc., **A223** (1954), p. 404.
9) Cottrell, A.H.: Trans. AIME, **212** (1958), p. 192.
10) Petch, N.J.: Phil. Mag., **3** (1958), p. 1089.
11) Kitajima, K.: Rep. Res. Inst. Appl. Mech., Kyushu Univ., **5**(1957), p. 87.
12) Low, J.R. Jr.: Progr. Mater. Sci., **12** (1963), p. 1.
13) Kitajima, K.: Proc. 1st Intl. Conf. Fracture (JSSFM 1966, Sendai), p. 659.
14) Hirsch, P.B.: Dislocation Dynamics (McGraw-Hill 1968, New York), p. 57, Phil. Mag., **8** (1963), p. 1895.
15) Suzuki, H.: Dislocation Dynamics (McGraw-Hill 1968, New York), p. 679.
16) Haasen, P.: Trans. JIM suppl., **9** (1968), XL.
17) Stroh, A.N.: Advanc. Phys., **6** (1957), p. 418.
18) Kitajima, K.: Proc. 1st Intl. Conf. Fracture (JSSFM 1966, Sendai), p. 647, Bullet. Res. Inst. Appl. Mech. Kyushu Univ. No. 19, (1962) p. 1, (in Japonese)
19) Cottrell, A.H., Kelly, A.: Endeavour, **25** (1966), p. 27.
20) Brenner, S.S.: J. Appl. Phys., **27** (1956), p. 62.
21) Hull, D.: Proc. 1st Intl. Conf. Fracture (JSSFM 1966 Sendai), p. 629, Phil. Mag., **161** (1969), p. 951.
22) Mackenzie, J.K.: Thesis Bristol (1949), Seeger, A.: Handb. der Phys., **VII-2** (1958), p. 7.
23) Cohen, J.B. et al.: Acta. Met., **10** (1962), p. 894, Crussard. C.: Compt. Rend., **252** (1961), p. 273.
24) Born, M.: Proc. Camb. Phil. Soc., **36** (1940), p. 160, p. 454.
25) Kelly, A., Tyson, W.R., Cottrell, A.H.: Phil. Mag., **15** (1967), p. 567. Tyson, W.R.: Phil. Mag., **14** (1966): p. 925.
26) Zwicky, F.: Z. Phys., **24** (1923), p. 131.
27) Wakoh, S., Yamashita, J.: J. Phys. Soc. Japan, **21** (1966), p. 1712. Mott, N. F.: Adv. Phys., **13** (1964), p. 325.
28) Johnson, R.A.: Phys. Rev., **134A** (1964), p. 1329.
29) Chang, R.: Fracture (Chapman & Hall 1969, London), p. 306.
30) I. Ichikawa, S. Mizushima, Rep. JIM, Vol. 8, (1969) p. 384, (in Japanese)
31) Friedel, J. et al.: J. Phys. Chem. Solids, **25** (1964), p. 781.
32) Hume-Rothery, W.: Progr. Material Sci., **13** No. 5 (Pergamon 1967, New York), p. 229.
33) Leslie, W.C.: Trans. ASM, **62** (1969), p. 690.
34) Christian, J.W.: 2nd Intl. Conf. Strength Metal Alloys, ASM (1970), p. 31.
35) Takeuchi, S. Yoshida, H., Taoka, T.: Trans. JIM **9** (1968), p. 715.
36) Nakada, Y., Keh, S.: Acta Met., **16** (1968), p. 903.
37) Sato, A.: Ph. D. Dissertation, Northwestern Univ. (1971), Proc. 2nd Intl. Conf. Strength Metal Alloys, Calif. (1970).
38) A. Sato, M. Meshii, Acta Met., **21** (1973) p. 753.
39) K. Kitajima, H. Abe, N. Tsukuda, Rep. Res. Inst. Appl. Mech., Kyushu Univ., **70** (1975) p.
40) Jolly, W.: Trans. AIME, **242** (1968), p. 306.
41) Floreen, S., Hayden, H.W.: Trans. AIME, **239** (1967).
42) Kaufman, L., Cohen, M.: Progress in Metal Physics, Vol. 7 (1958), p. 165.

* References after 1971 are added in the translation.

43) Terasaki, F.: Acta. Met., **15** (1967), p. 1057.
44) Hull, D.: Acta. Met., 8 (1960), p. 11, Honda, R.: Proc. 1st Intl. Conf. Fracture (JSSFM 1966, Sendai) p. 615.
45) Kitajima, K., Futagami K.: Electron Microfractography, ASTM STP No 453, (1969), p. 33.
46) Cottrell A.H.: NPL Symp. Relation Structure Strength Metals Alloys, 1963, p. 456.
47) Friedel, J.: Fracture, Swampscott (MIT 1959, New York), p. 498.
48) Tetelman, A.F.: Fracture of Solids, (Intersc. Publ. 1963, New York), p. 461.
49) Gilman, J.J.: Proc. 1st Intl. Conf. Fracture, (JSSFM 1966, Sendai) p. 733.
50) Gilman, J.J.: Trans· AIME, **209** (1957) p. 449.
51) Kitajima, K.: Intl. Conf. Mech. Behav. Mater., Kyoto (1971).
52) Crussard, C., Borione, R., Plateau, J., Morillon, Y., Maratray, F.: J. Iron Steel Inst., **183** (1956), p. 146.
53) Yamamoto, M., Takahashi, S., Rep. Brittle Fracture of Steels, No. 129 Committee, Japan Science Foundation (1966) p. 209, (in Japanese).
54) Reinbolt, J.A., Harris, W.J., Jr., Trans. ASM, **44** (1952) p. 225.
55) Allen, N.P.: J. Iron Steel Inst., **174** (1953), p. 108.
56) McMahon, C.J., Cohen, M.: Proc. 1st Intl. Conf. Fracture, (JSSFM 1966, Sendai) p. 779.
57) Hahn, G.T., Averbach, B.L., Owen, W.S., Cohen, M.: Fracture, Swampscott, (MIT 1959, New York), p. 91.
58) Averbach, B.L.: Proc. 1st Intl. Conf. Fracture, (JSSFM 1966, Sendai) p. 747.
59) Yokobori, T.: Tech. Rep. Tohoku Univ., Vol. **28** (1964), p. 167.
60) Ashby, M.F.: Phil. Mag., **21** (1970), p. 399.
61) Koshiga, F., Rep. Brittle Fracture of Steels, No. 129 Committee, Japan Science Foundation, (1966) p. 383.
62) Low, J.R.: The Fracture of Metals, Prog. Mater. Sci., **12** No. 1 (1963), p. 1.
63) Roesch, L., Henry, G.: Electron Microfractography, ASTM STP No. 453, (1969), p. 3.
64) Green, A.P., Hundy, B.B.: J. Mech. Phys. Solids, **4** (1956), p. 128.
65) Hendrikson, J.A. et al.: Trans. ASM, **50** (1958), p. 656.
66) Knoff, J.F.: Fracture, Brighton, (Chapman & Hall 1969, London), p. 205.
67) Kanazawa, T., Machida, S., Momota, S., Hagiwara, Y.: Fracture, Brighton, (Chapman & Hall 1969, London), p. 1.
68) Kanazawa, T., Strength and Fracture of Metals (Maruzen 1964, Tokyo) p. 197, (in Japanese).
69) Koshiga, F., Imasawa, O., Takehana, S., Trans. Japan Inst. Naval Arch., No. 114, (1963), (in Japanese).
70) Ikeda, K., Rep. Brittle Fracture of Steels, No. 129 Committee Japan Science Foundation, (1966) p. 256, (in Japanese).
71) Rhode, R.W.: Acta Met., **17** (1969), p. 352.
72) Hall, E.O.: Mech. Phys. Solids, **1** (1953), p. 227.
73) Rosenfield, A.R., Pai, P.K., Hahn, G.T.: Proc. 1st Intl. Conf. Fracture, (JSSFM 1966, Sendai), p. 223.
74) Suhara, J., Suhara, T.. Kitajima, K.. Tsuji, I., Rep. 2nd. Research Committee Strength of Steels, (1965), (in Japanese).
75) Minami, F., Kuramoto, E., Takeuchi, S.: Phys. stat. sol., (a) 12 (1972) p. 581, (a) 22 (1974), p. 81, p. 411, Duesbery, M.S., Vitek, V., Bowen, D.K.: Proc. Roy. Soc., A 332 (1973), p. 85.

(Received December 27, 1974)